It is advisable to refer to the publisher's version if you intend to cite from the work. See Guidance on citing.

To link to this article DOI: http://dx.doi.org/10.1088/2515-7620/ad578c

Publisher: IOP Science

www.reading.ac.uk/centaur

CentAUR

Central Archive at the University of Reading

Reading's research outputs online

INCLUSIVE PUBLISHING
TRUSTED SCIENCE

LETTER • OPEN ACCESS

Role of tidal mixing on ocean exchange through the Strait of Hormuz

View the article online for updates and enhancements.

Environmental Research Communications

Role of tidal mixing on ocean exchange through the Strait of Hormuz

Mohammed Salim[1,2] ⓘ, Subeesh M P[1,3,4], Jeffery Scott[5], Hajoon Song[6,7], John Marshall[5] and
Maryam R Al Shehhi[1] ⓘ

[1] Department of Civil Infrastructure and Environmental Engineering, Khalifa University of Science and Technology, Abu Dhabi, United Arab Emirates
[2] Department of Meteorology, University of Reading, United Kingdom
[3] MARUM—Center for Marine Environmental Science, University of Bremen, Bremen, Germany
[4] Institute of Environmental Physics, University of Bremen, Bremen, Germany
[5] Earth, Atmospheric and Planetary Science Department, Massachusetts Institute of Technology, 77 Massachusetts Ave., Cambridge, MA 02139, United States of America
[6] Department of Atmospheric Sciences, Yonsei University, Seoul, Republic of Korea
[7] Division of Environmental Science & Engineering, Pohang University of Science and Technology, Pohang, Republic of Korea

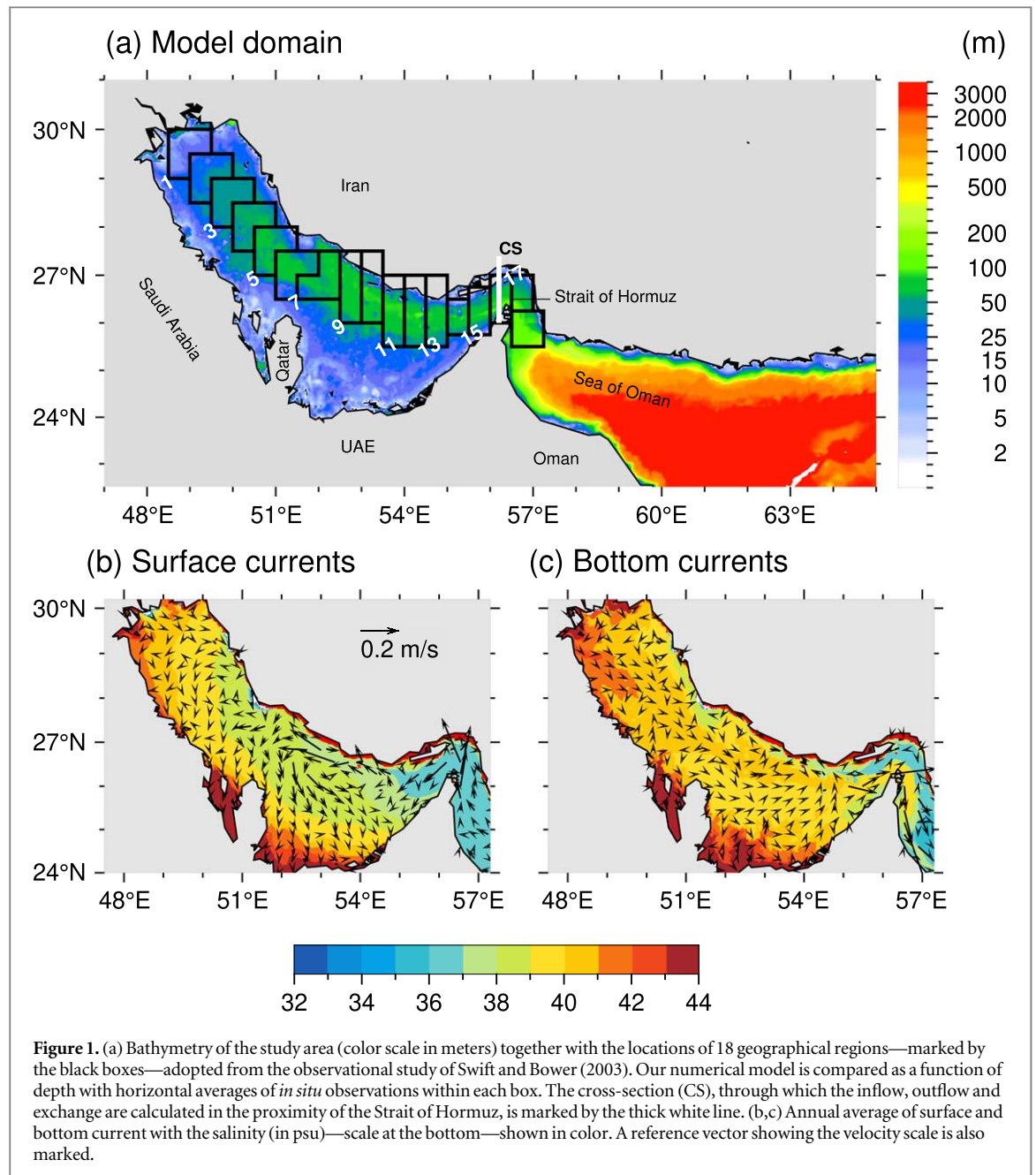**E-mail:** maryamr.alshehhi@ku.ac.ae

Abstract

We investigate the influence of tides on the exchange of water between the Arabian Gulf and the Sea of Oman through the Strait of Hormuz using a high-resolution numerical model. Two numerical simulations are contrasted, one with and one without tidal forcing. We find that tides suppress exchange through the Strait, by ∼20% in the annual mean, being largest in the summer (∼30%) and diminishing in the winter (∼13%). Tides enhance the parameterised shear-driven vertical mixing inside the Gulf and Strait, mixing warm, relatively fresh surface waters downward thus reducing the density of bottom waters flowing outwards. This reduces the lateral difference of density between Gulf and Sea of Oman and hence the exchange through the Strait. Maximum reductions occur in summer when both the vertical stratification and mixing is the largest.

Plain language summary

In a modeling study we explore how tides affect the exchange of water between the Arabian Gulf and the Sea of Oman through the Strait of Hormuz. We find that tides reduce the exchange by roughly 20% in the annual mean, the effect being greatest and reaching 30% in the summer. Tides enhance the mixing of warm, fresh surface waters downwards in the water column, reducing the density of bottom waters inside the Gulf. This results in a diminution of the gross density difference between the Gulf and the Sea of Oman and hence reduces the exchange. The effect is most pronounced in the summer when Gulf waters are the most stratified and mixing the greatest. We conclude that the realism of ocean models of the Gulf will be greatly enhanced if they explicitly represent tides and their associated mixing.

1. Introduction

The Arabian Gulf (AG) is a shallow basin located between the northern boundary of the Arabian Peninsula and Iran, figure 1(a). Its ocean is one of the most saline in the world (figures 1(b), (c)). Due to its arid climate, evaporation exceeds freshwater input, and is compensated by a net surface inflow through the narrow Strait of Hormuz (SH) (Alosairi *et al* 2020, Privett 1959, Johns *et al* 2003, Xue and Eltahir 2015). In compensation, warm, saline and oxygenated waters residing at shallow depths of the AG, exit lower down the water column through the Strait (figure 1(b)). These spread at intermediate depths into the Arabian Sea and the Bay of Bengal,

Figure 1. (a) Bathymetry of the study area (color scale in meters) together with the locations of 18 geographical regions—marked by the black boxes—adopted from the observational study of Swift and Bower (2003). Our numerical model is compared as a function of depth with horizontal averages of *in situ* observations within each box. The cross-section (CS), through which the inflow, outflow and exchange are calculated in the proximity of the Strait of Hormuz, is marked by the thick white line. (b,c) Annual average of surface and bottom current with the salinity (in psu)—scale at the bottom—shown in color. A reference vector showing the velocity scale is also marked.

ultimately significantly affecting the hydrography of the north Indian Ocean (Jain *et al* 2017, Sheehan *et al* 2020, Pous and Lazure 2004a, Pous *et al* 2004b). AG water plays a significant role in the ventilation of the oxygen minimum zone of the Arabian Sea (McCreary *et al* 2013). Understanding the mechanism behind AG water outflow through the SH is thus of great importance. An improved understanding of water mass transport between the AG and Sea of Oman may also better inform efforts to preserve the marine environments of the region.

Many modelling and observational studies have addressed the circulation of the AG and the characteristics of the water mass exchange through the SH (Thoppil and Hogan 2010a, Johns *et al* 2003, Pous and Lazure 2004a, Pous *et al* 2015, Lorenz *et al* 2021, Kämpf and Sadrinasab 2006, Reynolds 1993a). The circulation of the AG is broadly cyclonic and the SH plays an important role in restricting the exchange between the Gulf and Sea of Oman (Reynolds 1993a, Emery 1956, Brewer and Dyrssen 1985, Hunter 1983, Reynolds1993, Chao *et al* 1992, Johns *et al* 2003). These studies have explored the various processes at work that control exchange. Swift and Bower (2003) suggest that changes in sea surface slope between the Sea of Oman and the AG is the primary driving force of exchange on synoptic time scales. Thoppil and Hogan (2010a) and Vasou *et al* (2020) noted that such short timescale variability is set by the local winds. According to Vasou *et al* (2020), short-term variability (2 to 5 day) in transport shows a quasi-barotropic pattern affecting mostly the upper layers. On longer time scales (seasonal to interannual), exchange through the SH is thought to be controlled by the horizontal density gradient

between the inner Gulf and the Sea of Oman (Pous *et al* 2015, Chao *et al* 1992, Yao and Johns 2010, Thoppil and Hogan 2010a, Kämpf and Sadrinasab 2006).

Studies have suggested that mixing within the AG is associated with strong tidal currents, topographic features and eddy activity (Lorenz *et al* 2021, Swift and Bower 2003). However, previous studies of water mass exchange through the SH have disregarded the role of tides in the time-mean general circulation, assuming that its affect is small when averaged over periods longer than a few tidal cycles (Pous *et al* 2012, Hughes and Hunter 1979). The one exception of which we are aware is the recent study of Campos *et al* (2022) who find, as here, that inclusion of tides significantly reduces exchange. However, they did not explore underlying mechanisms. Studies in different Straits indeed find that diapycnal mixing and residual currents induced by tides can play a significant role in water mass modification and the large-scale circulation (Koch-Larrouy *et al* 2007, Nagai and Hibiya 2015) by affecting inflow and outflow (Farmer and Armi 1986, Naranjo *et al* 2014, Sannino *et al* 2004, 2015, Kurogi and Hasumi 2019). In this study, then, we follow on from the work of Campos *et al* (2022) and focus in on the underlying mechanisms at work. We employ a high resolution 3D model of the AG previously reported in Al-Shehhi *et al* (2021) and contrast solutions with and without tidal forcing.
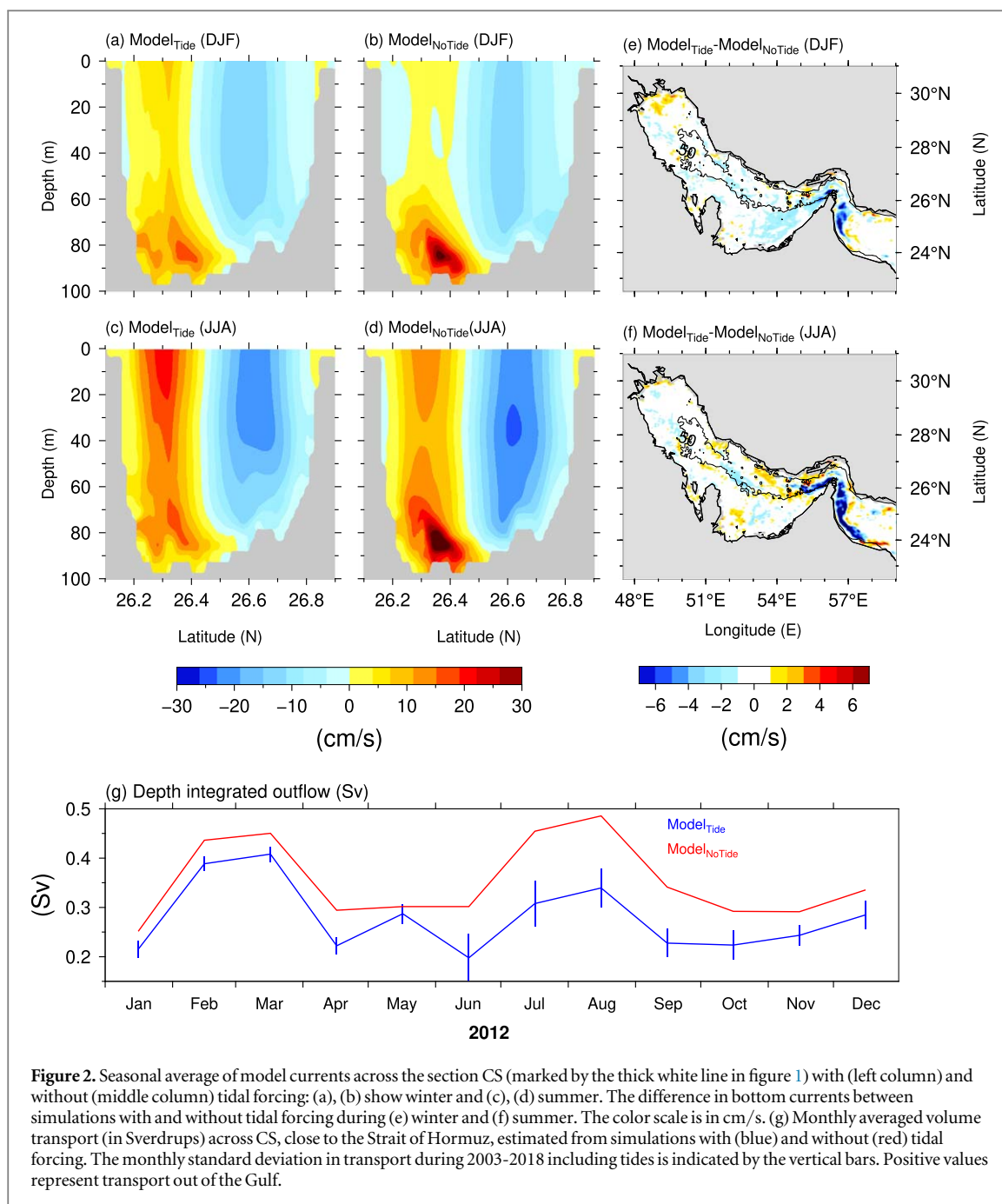
2. A high resolution model of the Arabian Gulf based on MITgcm

We make use of a high-resolution configuration of the MITgcm (Marshall *et al* 1997) deployed for the Arabian Gulf as described in Al-Shehhi *et al* (2021). The MITgcm has been extensively used in studies of tides, internal tides, and residual currents in coastal waters in the presence of complex topographies and geometries—see, for example, (Sannino *et al* 2015, Wang *et al* 2015). The model is configured for the AG and Sea of Oman (23.2°N to 30.7°N and 47.3°E to 62.3°E) as shown in figure 1(a). It is driven by meteorological forcing at its upper surface, from tides prescribed at its open-ocean lateral boundaries and by river inflow along the coasts. It has a high horizontal spatial resolution of approximately 2.5 km and 83 vertical levels ranging from 1 m in thickness at the surface to ~200 m at the bottom out in the Sea of Oman. More details can be found in Al-Shehhi *et al* (2021). A high-resolution bathymetry dataset derived from Smith and Sandwell (1997) is used with a resolution of 3 km. The model is adjusted so that evaporation over the AG is compensated by freshwater fluxes from the lateral boundary (E-P-R; where E is Evaporation, P is Precipitation and R River run-off). A standard configuration of the nonlocal K-profile parameterization (KPP) (Large *et al* 1994, 1997) is used to parameterize ocean turbulent mixing.

The temperature, salinity and velocity components for initial and lateral boundary conditions are obtained from a 1/48° MITgcm global model simulations known as LLC4320 (Rocha *et al* 2016). The model was forced at the surface by 6-h European Centre for Medium-Range Weather Forecasts (ECMWF) atmospheric operational model analysis at 0.148° resolution (~15 km). A custom monthly river freshwater outflow dataset (capturing the discharge of the Shatt Al-Arab, Mand, Hindijan, and Hilieh rivers) is also included obtained from Large and Nurser (2001) and as described in Al-Shehhi *et al* (2021).

The amplitude and phase of seven tidal constituents (M2, S2, N2, K2, K1, O1 and P1) obtained from the Arabian Sea regional barotropic tidal model, OSU Tidal Inversion Software (OTIS) (Egbert *et al* 1994, Egbert and Erofeeva 2002), are prescribed along the open boundaries. The model's fidelity in capturing tidal patterns and amplitudes is assessed in the supplementary material, where it is compared with observations from tide gauges. The spatial distribution of the four major tidal constituents is also presented there. The model effectively captures tidal features, consistent with previous studies (Mashayekh Poul *et al* 2016, Pous *et al* 2012, Hyder *et al* 2013, Madah and Gharbi 2022). The M2 tide is the most dominant constituent in the Gulf and Sea of Oman, followed by K1, S2, and O1. The co-tidal maps shows two amphidromic points for semi-diurnal tides: one in the southeastern Gulf near Abu Dhabi and another in the southwestern Gulf. Additionally, a diurnal tide amphidromic point is located in the south-central Gulf off Bahrain's coast (see supplementary). Here we focus on the impact of those tides on mixing and the general circulation, in particular exchange through the SH.

To study the effect of tides on the general circulation within the Gulf, we designed two numerical experiments driven by: (i) atmospheric forcing with no tides and (ii) both tides and atmospheric forcing. The model is integrated for the year 2012 in a repeating cycle. The model is run on for 6 years with repeating surface forcing and boundary conditions and the final year is used in analysis. We also carried out a multi-year calculation including tidal and atmospheric forcing from 2003 to 2018 to ensure that interannual variability does not affect our conclusion. We find that interannual variability in exchange through the SH is indeed small compared to the difference of transport due to the inclusion of tidal processes.

Figure 2. Seasonal average of model currents across the section CS (marked by the thick white line in figure 1) with (left column) and without (middle column) tidal forcing: (a), (b) show winter and (c), (d) summer. The difference in bottom currents between simulations with and without tidal forcing during (e) winter and (f) summer. The color scale is in cm/s. (g) Monthly averaged volume transport (in Sverdrups) across CS, close to the Strait of Hormuz, estimated from simulations with (blue) and without (red) tidal forcing. The monthly standard deviation in transport during 2003-2018 including tides is indicated by the vertical bars. Positive values represent transport out of the Gulf.

3. Comparing simulations with and without tides

3.1. The role of tides in the exchange through the Strait of Hormuz

We analysed our most realistic simulation which included tidal forcing (hereafter 'tidal run') and compared it to an additional calculation in which the tidal forcing is removed (hereafter 'non-tidal run'). The monthly volume transport through the cross-section CS (marked in figure 1(a)) are computed by integrating positive (outflow) and negative (inflow) values across the transect: see figure 2(g). In both tidal and non-tidal simulations, the volume transport shows similar seasonal variation peaking during late winter and again in summer. However, the magnitude of transport differs between them, with a yearly-averaged 20% reduction in the tidal case: the average outflow (inflow) is 0.278 (.285) Sv and 0.357 (0.352) Sv for tidal and non-tidal runs respectively. Seasonal-average values show that the volume transport is reduced by 30% in summer and 13% in winter. The standard deviation of volume transport across the Strait due to interannual atmospheric forcing is also indicated in figure 2(g). It is evidently small compared to the difference between tidal and non-tidal transport.

The annual mean transport estimated from our tidal run is closer to observational estimates than in the absence of tides. The annual mean volume transport through the Strait inferred from mooring observations (Johns *et al* 2003) is ~0.23 ± 0.04 Sv (inflow) and ~0.21 ± 0.05 Sv (outflow). Thus, including tides reduces the

tendency of our model to over-estimate the exchange between the AG and the Sea of Oman. Other modelling studies driven by tides from open boundaries are also broadly consistent with observed estimates of inflow (outflow), e.g. Pous *et al* (2015): 0.203 (0.194), Pous *et al* (2004b): 0.21 (0.17) and Vasou *et al* (2020): 0.22(0.15). That said, our results suggest that including tidal forcing is critical to obtaining a realistic representation of exchange through the Strait.

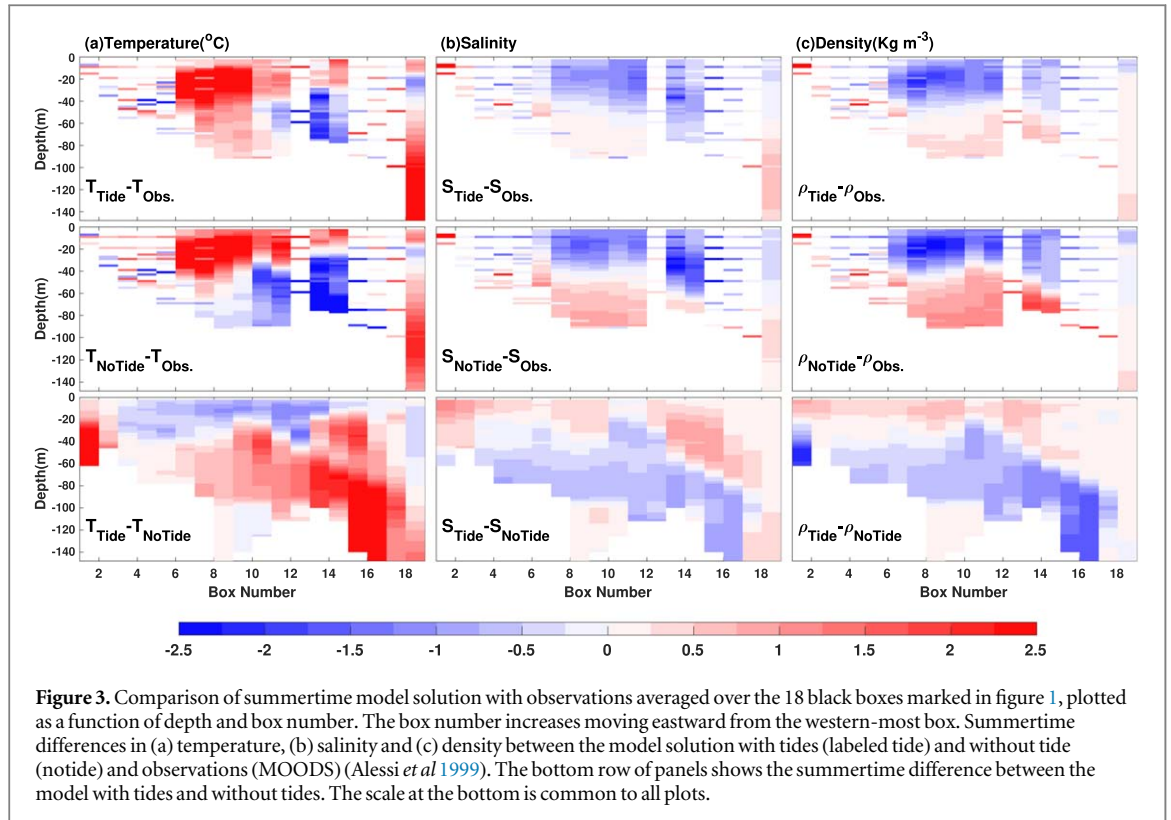### 3.2. Circulation driven with tides and atmospheric forcing

We examined a vertical cross section of the model's currents through the SH to understand the change in volume transport in tidal and non-tidal simulations. The currents are averaged for winter (DJF) and summer (JJA) and the zonal component of the current velocity is shown (see figures 2(a)–(d)) along the line CS. Positive values show outflow (red shading) and negative values inflow (blue). The inflow occurs through the northern half of the Strait and outflow through the southern half. In winter, the inflow is largely barotropic, but the outflow occurs predominantly at depths below 60 m, particularly in the non-tidal run where bottom currents peak at order 30 cm s^{-1}. Without tides the outflow is weak in the southern half of the Strait at depths shallower than 60 m, even exhibiting slight inflow along the southern coast (largely absent from the tidal run). In summer, however, differences are more pronounced. Without tides, inflow remains fairly uniform in the vertical, while outflow is largest at depth. However, with tides both inflow and outflow are largest in the top 40 m of the Strait. Note that the bottom-intensified outflow remains fairly constant throughout the year, implying that the summer exchange peak is largely associated with the barotropic component in the absence of tides, but is surface intensified in the presence of tides.

To further compare tidal and non-tidal runs, we show the difference in bottom currents in a plan view of the AG (figures 2(e)–(f)). Tidal forcing suppresses currents at depth, extending out to the Sea of Oman through the SH. We also analyzed the larger-scale circulation to determine whether tidal influences are restricted to the SH or whether there are basin-wide changes—see the depth-averaged and surface currents plotted in supplementary figures S6 & S7. It is found that the tide has impact throughout the Gulf, and particularly along its northern coast. The largest difference between tidal and non-tidal runs is found in the Gulf, to the west of Siri Island close to the SH, where depth average speed differences reach 21 cms^{-1} and 25 cms^{-1} in winter and summer respectively. The maximum residual current speeds in the SH during summer are 20 cms^{-1} and 33 cms^{-1} for tidal and non-tidal runs respectively, during winter 29 cms^{-1} and 32 cms^{-1}. In addition to the effect of tides on current speeds, tidal forcing significantly affects flow patterns. The north-westward flowing Iranian Coastal Current (ICC), which is associated with density gradients between the AG and the Sea of Oman (Swift and Bower 2003, Thoppil and Hogan 2010b), is prominent during both winter and summer in the non-tidal run. The weaker ICC in winter is attributed to the reduced density gradient between the Sea of Oman and the AG due to winter cooling effects. The addition of tidal forcing weakens and modifies the ICC in all seasons. The summer and winter circulation patterns (see supplementary figure S6) both show that the tide induces a large change in circulation. The addition of tides expands the gyre and its strength is significantly reduced in winter. The major tidal modifications on circulation patterns occur within the Gulf, predominantly to the north where the bathymetry is deeper and most sharply changing.

3.3. Effect of tides on hydrography

The above results show that tidal forcing significantly modifies the basin wide circulation, with substantial reduction in deep currents in the SH. As noted in previous studies, the density gradient between the AG and the Sea of Oman is the dominant force driving seasonal circulation in the Gulf (Yao and Johns 2010, Kämpf and Sadrinasab 2006, Thoppil and Hogan 2010b). Any change in this gradient may affect the basin-wide circulation and exchange through the Strait. In order to understand whether tidal forcing has any role in hydrographic structure, and thereby circulation and exchange, we analyzed the temperature and salinity distributions in tidal and non-tidal simulations.

We first compared seasonal-means of temperature, salinity and density with historical observations from the Master Oceanographic Observations Dataset (MOODS) (Alessi *et al* 1999) which spans the 1940-1990 period. Al-Shehhi *et al* (2021) compared the seasonal-average hydrography obtained from the tidal run used in this study with the same MOODS observations. Here we extend this comparison to the non-tidal simulation. We take 18 boxes along the center of the AG from its north-west corner to the Sea of Oman, and horizontally average the hydrography from the non-tidal run for summer (see figure 3) and winter (see supplementary figure S8). The boundaries of the boxes (see figure 1(a)) are defined following Swift and Bower (2003). Comparing tidal and non-tidal runs with observations (upper rows of figures 3 & S8), we see that both have similar biases, specifically a too warm and fresh bias toward the surface (i.e. too light) and too cold and salty at depth (i.e. too dense). However, these biases are less pronounced in the tidal simulation. This can be seen most clearly when we compare the density (right column): the tidal run remains modestly too light at the surface (i.e. remains too

Figure 3. Comparison of summertime model solution with observations averaged over the 18 black boxes marked in figure 1, plotted as a function of depth and box number. The box number increases moving eastward from the western-most box. Summertime differences in (a) temperature, (b) salinity and (c) density between the model solution with tides (labeled tide) and without tide (notide) and observations (MOODS) (Alessi *et al* 1999). The bottom row of panels shows the summertime difference between the model with tides and without tides. The scale at the bottom is common to all plots.
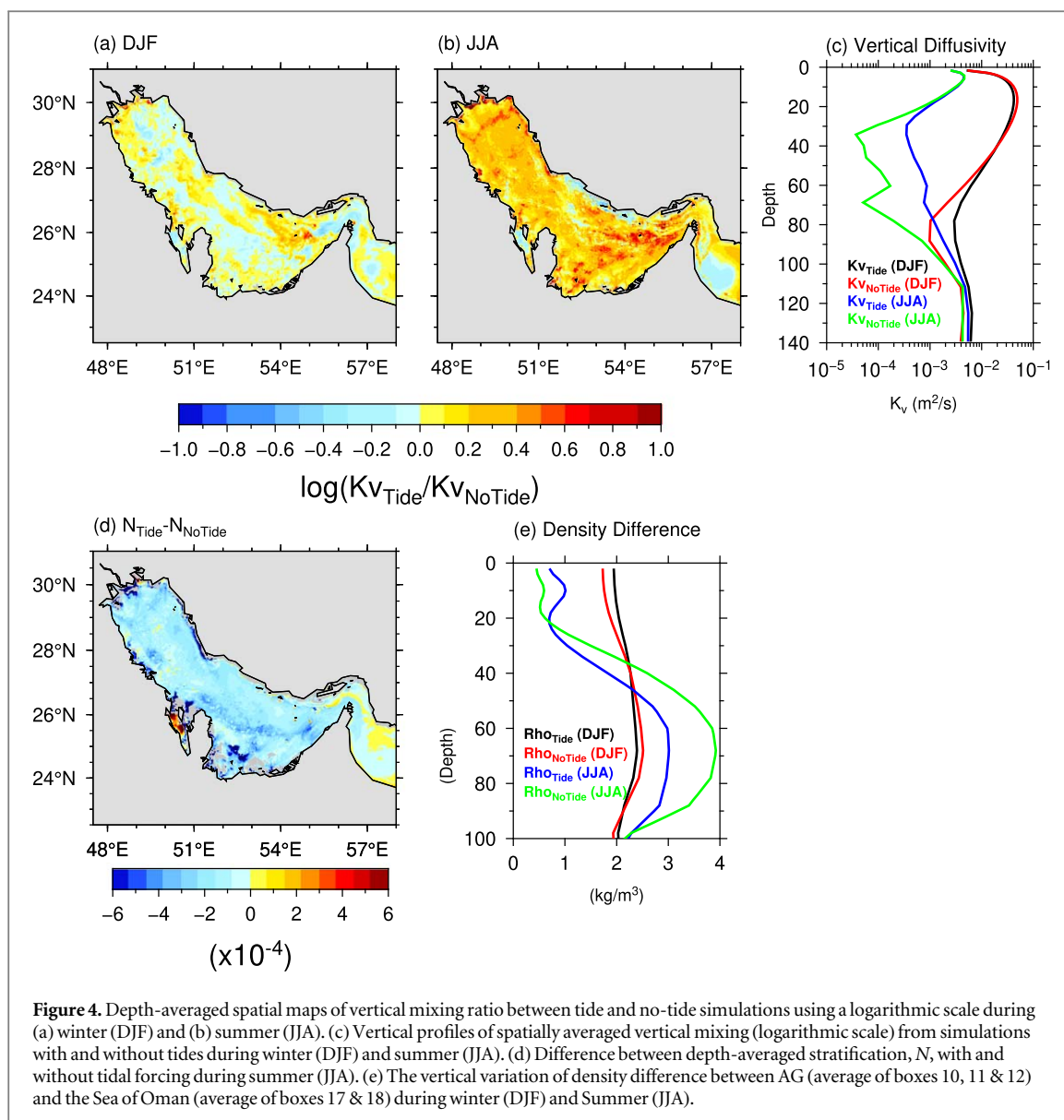
warm and fresh), but exhibits minimal bias at depth. The bottom water density is significantly reduced in the tidal run. During winter, the densities in both the tidal and non-tidal simulations are closer to observations. The non-tidal run shows a difference of 1 kgm^{-3} with observation in summer, whereas the bias is 0.3 kgm^{-3} in the presence of tides. In summary, summer biases in temperature, salinity and density are considerably reduced in the presence of tides.

The simulated spatial distribution of bottom temperature, salinity and density differences during DJF and JJA is presented in the supplementary materials (see figure S9 in the supplementary section). Tidal forcing is felt across the entire basin in both AG and SH with a strong influence during the summer (JJA) months. The box-average difference between tidal and nontidal runs over the AG (47.3^oE: 56^oE, 23.2^oN: 30.7^oN) is found to be 0.25 °C and 0.43 °C during winter and summer respectively. The AG bottom water is freshened by 0.26 (0.5) psu in winter (summer) in the presence of tides. Waters on the southern coast of the AG (UAE) are more saline, and dense water to the south is more saline than dense water to the north. A similar observation was made by Swift and Bower (2003). The decrease in salinity and increase in temperature decreases the bottom density basin wide. The AG is strongly stratified by temperature during summer, with a weaker salinity increase with depth (Al-Shehhi *et al* 2021). In the presence of tides, bottom temperatures in the SH (56^oE: 57^oE, 25.8^oN: 27.5^oN) exhibit a larger increase of 0.6 °C in winter and 0.9 °C in summer than without tides. The salinity in the presence of tides is decreased at the bottom. In summary, tidal-induced mixing acts to cool and increase salinity at the surface, and warm and freshen at depth.

3.4. Vertical mixing

To infer the vertical mixing due to tides, we compared the model-derived vertical (diapycnal) mixing in the two simulations. The depth-averaged vertical mixing (Kv, figures 4(a) & (b)) is distinctly elevated relative to without tides in summer in the AG. The vertical profile of mixing, figure 4(c), shows a higher Kv with tides between depths of 20 m and 110 m in summer and 60 m to 100 m in winter. In the SH, the Kv with tides is elevated by a factor of 4 and 1.5 in summer and winter, respectively. This suggests that the vertical mixing of tracers is significantly enhanced in the presence of tides. Figure 4 also shows the ratio between the vertical mixing (tide and notide) for winter and summer. In summer tidal mixing is found throughout the domain, i.e. it is more significant in the presence of stratified waters and so summer water masses are more influenced by the tides than in winter. The buoyancy frequency ($N = \sqrt{-\frac{g}{\rho}\frac{d\rho}{dz}}$, where ρ is the potential density) also documents the weakening of the stratification with tides (figure 4). The spatial distribution shows that the difference between

Figure 4. Depth-averaged spatial maps of vertical mixing ratio between tide and no-tide simulations using a logarithmic scale during (a) winter (DJF) and (b) summer (JJA). (c) Vertical profiles of spatially averaged vertical mixing (logarithmic scale) from simulations with and without tides during winter (DJF) and summer (JJA). (d) Difference between depth-averaged stratification, *N*, with and without tidal forcing during summer (JJA). (e) The vertical variation of density difference between AG (average of boxes 10, 11 & 12) and the Sea of Oman (average of boxes 17 & 18) during winter (DJF) and Summer (JJA).

the two simulations (tide—notide) is generally negative everywhere in the AG and SH. The maximum weakening of the stratification occurs during the summer period.

To study the impact of tidal mixing on horizontal density gradients we estimated the average density between two boxes, one inside the AG (average of Boxes 10, 11 & 12) and a second box outside the SH, in the Sea of Oman (average of Boxes 17 & 18). Figure 4(e) shows the vertical profiles of this difference in the summer (JJA) and winter (DJF) seasons, comparing tidal and non-tidal simulations. In the presence of tides we see a notable reduction of this difference in the summer, particularly between depths of 40 m and 90 m. In contrast this effect is considerably weaker in winter. The mixing of lighter waters downwards due to tides is thus seen to decrease the horizontal density difference. In winter, the tide has little effect on these gradients. The reduced density gradient between the AG and Sea of Oman in the presence of tides is likely an important factor in the significant suppression of deep water outflow in summer.

4. Summary and conclusions

We investigated the impact of tides on the exchange between the AG and the Sea of Oman through the Strait of Hormuz (SH) by comparing high resolution numerical experiments with and without tidal forcing. The reliability of the tides simulated in the model is assessed—as set out in the supplementary material—by comparing the model with time series observations from coastal tide gauges and current meters. We find that the tide modifies basin-wide circulation and impacts the properties and volume flux of deep water outflow through the SH (figures 2(f) & (g)). The outflow (and compensating inflow) is suppressed in the presence of tides by 20%

in the annual mean, by 30% in summer and 13% in winter (figure 2(a)). This broadly confirms the recent study of Campos *et al* (2022) who used a different model.

Earlier studies have shown that barotropic tides can induce residual currents in the Gulf due to the non-linear interaction of large-amplitude tidal currents with bathymetry: the M2 residual itself can exceed 0.15 ms^{-1} in the AG—see Poul *et al* (2016). Some large-scale circulation changes found in our model may thus be associated with such residuals. However, the primary reason for large-scale changes, we believe, is due to the presence of enhanced vertical mixing induced by the tides.

We find that mean bottom currents are significantly suppressed in the presence of tides due to the modification of the hydrographic structure inside the Gulf. The deep waters in the SH are warmed by 0.7 °C and freshened by 0.62 psu (average of summer and winter months) when tides are included (see figure 3 and supplementary figure S8), indicative of enhanced downward vertical mixing of lighter surface waters. The increase in bottom temperature is larger in summer than winter, and is associated with stronger summertime tidal mixing. The reduction of basin-wide stratification also confirms elevated vertical mixing rates with tides. Enhanced shear-driven mixing, especially in summer, reduces the density of the bottom water within the AG, reduces the lateral density between the AG and Oman Sea and, concomitantly, the rate of lateral exchange. The effect is weaker in the winter than in the summer. Indeed the AG is well mixed in winter and so the role of tides in setting deep water outflow is much reduced.

The spatial distribution of vertical mixing shows large values in the vicinity of topography features such as small seamounts and shelf-slope regions (figure 4). Tide-topography interaction and generation of internal tides is one of the important processes of enhancing mixing. The greater stratification in summer, together with the presence of many topographic features, facilitates strong internal tides and enhanced mixing. The bottom water modification due to tide-topography interaction also occurs elsewhere in the ocean—see, e.g., the Jithin and Francis (2020) study of warm bottom waters in the Andaman Sea of the north-eastern Indian Ocean. Recently (Kurogi and Hasumi 2019) also noted the tidal suppression of through-flow in a narrow Strait of Seto Inland Sea, Japan. Our key result should be contrasted with, for example, Naranjo *et al* (2014) who found outflow increases significantly in the Strait of Gibralter by 28% to 33% annually in the presence of tides.

The AG is known for its markedly distinct winter and summer characteristics, primarily due to significant seasonal shifts in temperature and salinity (T/S properties). Despite these marked variations in T/S properties, they are not prominently reflected in the exchange rates through the SH (Johns *et al* 1998, Swift and Bower 2003). We find that tidal suppression in summer is the major factor maintaining a steady exchange. Our study suggests that both winter and summer water masses respond differently to tides. The tide significantly suppresses the through-flow of stratified summer water and hence controls the density driven circulation/exchange.

Climate change projections show that the AG may undergo substantial warming with perhaps adverse effects on marine ecosystems (Field and Barros 2014, Paparella *et al* 2022). The summer SST of AG could increase by perhaps 4 °C or so by 2100 (Noori *et al* 2019), leading to an increase in stratification as the upper ocean warms. It would be interesting to know whether increased stratification due to this warming enhances the baroclinic tide and its associated mixing or reduces mixing due to the increased stratification. Whatever happens, future increased warming may affect exchange flows between the AG and the Sea of Oman due to the modulation of mixing from tides/internal tides acting on seasonally stratified Gulf waters.

Data availability statement

The Model (MIT-gcm) setup with compile-time and run-time parameters can be found at http://cvs.mitgcm.org/viewvc/MITgcm/MITgcm_contrib/llc_hires/llc_4320/. The Master Oceanographic Observations Dataset (MOODS), utilized in this study, originates from Alessi *et al* (1999). Tidal amplitude and phase data, derived from tide gauge observations, were obtained from Pous *et al* (2012), with the original source being the International Hydrographic Office. Current data from mooring stations, as cited in Reynolds (1993a), are

publicly available at NOAA National Oceanographic Data Center https://nodc.noaa.gov/archive/arc0001/9600082/1.2/data/.

ORCID iDs

Mohammed Salim ⓘ https://orcid.org/0000-0003-2854-503X
Maryam R Al Shehhi ⓘ https://orcid.org/0000-0003-1468-5875

References

Alessi C A, Hunt H D and Bower A S 1999 Hydrographic Data from the U.S. Naval Oceanographic Office: Persian Gulf, Southern Red Sea, and Arabian Sea 1923-1996 *Tech. Rep.* Woods Hole Oceanographic Institution MA

Alosairi Y, Alsulaiman N, Rashed A and Al-Houti D 2020 World record extreme sea surface temperatures in the northwestern Arabian/Persian gulf verified by in situ measurements *Mar. Pollut. Bull.* **161** 111766

Al-Shehhi M R, Song H, Scott J and Marshall J 2021 Water mass transformation and overturning circulation in the Arabian Gulf *J. Phys. Oceanogr.* **51** 3513–27

Brewer P G and Dyrssen D 1985 Chemical oceanography of the Persian Gulf *Prog. Oceanogr.* **14** 41–55

Campos E J, Kjerfve B, Cavalcante G, Vieira F and Abouleish M 2022 Water exchange across the Strait of Hormuz. Effects of tides and rivers runoff *Regional Studies in Marine Science* **52** 102336

Chao S-Y, Kao T W and Al-Hajri K R 1992 A numerical investigation of circulation in the Arabian Gulf *Journal of Geophysical Research: Oceans* **97** 11219–36

Egbert G D, Bennett A F and Foreman M G G 1994 TOPEX/POSEIDON tides estimated using a global inverse model. *Journal of Geophysical Research: Oceans* **99** 24821–52

Egbert G D and Erofeeva S Y 2002 Efficient inverse modeling of barotropic ocean tides *J. Atmos. Oceanic Technol.* **19** 183–204 (https://journals.ametsoc.org/view/journals/atot/19/2/1520-0426_2002_019_0183_eimobo_2_0_co_2.xml)

Emery K O 1956 Sediments and water of Persian Gulf *AAPG Bull.* **40** 2354–83

Farmer D M and Armi L 1986 Maximal two-layer exchange over a sill and through the combination of a sill and contraction with barotropic flow *J. Fluid Mech.* **10**

Field C B and Barros V R 2014 *Climate Change 2014-Impacts, Adaptation and Vulnerability: Regional Aspects* (Cambridge University Press)

Hughes P and Hunter J R 1979 A proposal for a physical oceanography program and numerical modeling of the KAP region *UNESCO Rep. Mar. Sci.* **27** Project for KAP 2/2

Hunter J R 1983 A review of the residual circulation and mixing processes in the Kuwait Action Plan Region, with reference to applicable modelling techniques *Proc. Symp. Workshop on Oceanographic Modelling of the Kuwait Action Plan, Dhahran* **28** 37–45

Hyder P *et al* 2013 Evaluating a new NEMO-based Persian/Arabian Gulf tidal operational model *Journal of Operational Oceanography* **6** 3–16

Jain V *et al* 2017 Evidence for the existence of Persian Gulf water and Red Sea water in the Bay of Bengal *Clim. Dyn.* **48** 3207–26

Jithin A and Francis P 2020 Role of internal tide mixing in keeping the deep Andaman Sea warmer than the Bay of Bengal *Sci. Rep.* **10** 11982

Johns W, Yao F and Olson D 1998 Observations of seasonal exchange through the Strait of Hormuz *Oceanography* **11** 58

Johns W, Yao F, Olson D, Josey S, Grist J and Smeed D 2003 Observations of seasonal exchange through the Straits of Hormuz and the inferred heat and freshwater budgets of the Persian Gulf *Journal of Geophysical Research: Oceans* **108** C12

Kämpf J and Sadrinasab M 2006 The circulation of the Persian Gulf: a numerical study *Ocean Sci.* **2** 27–41

Koch-Larrouy A, Madec G, Bouruet-Aubertot P, Gerkema T, Bessières L and Molcard R 2007 On the transformation of Pacific water into indonesian throughflow water by internal tidal mixing *Geophys. Res. Lett.* **34** 4

Kurogi M and Hasumi H 2019 Tidal control of the flow through long, narrow straits: a modeling study for the seto inland sea *Sci. Rep.* **9** 11077

Large W G, Danabasoglu G, Doney S C and Mcwilliams J C 1997 Sensitivity to surface forcing and boundary layer mixing in a global ocean model: annual-mean climatology *J. Phys. Oceanogr.* **27** 2418–2447

Large W G, McWilliams J C and Doney S C 1994 Oceanic vertical mixing: a review and a model with a nonlocal boundary layer parameterization *Rev. Geophys.* **32** 363–403

Large W G and Nurser A G 2001 Ocean surface water mass transformation *International Geophysics* vol 77 (Elsevier) pp 317–36

Lorenz M, Klingbeil K and Burchard H 2021 Impact of evaporation and precipitation on estuarine mixing *J. Phys. Oceanogr.* **51** 1319–1333

Madah F and Gharbi S H 2022 Numerical simulation of tidal hydrodynamics in the Arabian Gulf *Oceanologia* **64** 327–45

Marshall J, Adcroft A, Hill C, Perelman L and Heisey C 1997 A finite volume, incompressible navier stokes model for studies of the ocean on parallel computers *Journal of Geophysical Research: Oceans* **102** 5753–66

Mashayekh Poul H, Backhaus J and Huebner U 2016 A description of the tides and effect of qeshm canal on that in the Persian Gulf using two-dimensional numerical model *Arabian J. Geosci.* **9** 1–11

McCreary J P, Yu Z, Hood R R, Vinaychandran P, Furue R, Ishida A and Richards K J 2013 Dynamics of the Indian-Ocean oxygen minimum zones *Prog. Oceanogr.* **112-113** 15–37

Nagai T and Hibiya T 2015 Internal tides and associated vertical mixing in the Indonesian archipelago *Journal of Geophysical Research: Oceans* **120** 3373–90

Naranjo C, Garcia-Lafuente J, Sannino G and Sanchez-Garrido J C 2014 How much do tides affect the circulation of the mediterranean sea? from local processes in the strait of gibraltar to basin-scale effects *Prog. Oceanogr.* (https://doi.org/10.1016/j.pocean.2014.06.005)

Noori R *et al* 2019 Recent and future trends in sea surface temperature across the Persian Gulf and Gulf of Oman *PLoS One* **14** e0212790

Paparella F, D'Agostino D and Burt A J 2022 Long-term, basin-scale salinity impacts from desalination in the Arabian/Persian Gulf *Sci. Rep.* **12** 20549

Poul H M, Backhaus J, Dehghani A and Huebner U 2016 Effect of subseabed salt domes on tidal residual currents in the Persian Gulf *Journal of Geophysical Research: Oceans* **121** 3372–80

Pous C and Lazure X 2004a Hydrology and circulation in the Strait of Hormuz and the Gulf of Oman—Results from the GOGP99 Experiment: 1. Strait of Hormuz *Journal of Geophysical Research C: Oceans* **109** 42–56

Pous, Carton X and Lazure P 2004b Hydrology and circulation in the Strait of Hormuz and the Gulf of Oman—Results from the GOGP99 Experiment: 2. Gulf of Oman *Journal of Geophysical Research: Oceans* **109** C12038

Pous, Carton X and Lazure P 2012 A process study of the tidal circulation in the Persian Gulf *Open Journal of Marine Science* **2** 131–140

Pous, Lazure P and Carton X 2015 A model of the general circulation in the persian gulf and in the Strait of Hormuz: intraseasonal to interannual variabil ity *Cont. Shelf Res.* **94** 55–70

Privett D W 1959 Monthly charts of evaporation from the N. Indian Ocean (including the Red Sea and the Persian Gulf). *Quarterly Journal of the Royal Mete Orological Society* **85** 424–428

Reynolds R M 1993a Physical oceanography of the Gulf, Strait of Hormuz, and the Gulf of Oman—Results from the Mt Mitchell expedition *Mar. Pollut. Bull.* **27** 35–59

Rocha C B, Chereskin T K, Gille S T and Menemenlis D 2016 Mesoscale to Submesoscale Wavenumber Spectra in Drake Passage *J. Phys. Oceanogr.* **46** 601–20

Sannino G, Bargagli A and Artale V 2004 Numerical modeling of the semidiurnal tidal exchange through the Strait of Gibraltar *Journal of Geophysical Research: Oceans* **109** (C5) C05011

Sannino G, Carillo A, Pisacane G and Naranjo C 2015 On the relevance of tidal forcing in modelling the Mediterranean thermohaline circulation *Prog. Oceanogr.* **134** 304–29

Sheehan P M, Webber B G, Sanchez-Franks A, Matthews A J, Heywood K J and Vinayachandran P 2020 Injection of oxygenated Persian Gulf water into the southern Bay of Bengal *Geophys. Res. Lett.* **47** e2020GL087773

Smith W H F and Sandwell D T 1997 Global sea floor topography from satellite altimetry and ship depth soundings *Science* **277** 1956–62

Swift S A and Bower A S 2003 Formation and circulation of dense water in the Persian/Arabian gulf *Journal of Geophysical Research C: Oceans.* **10(C1)** 4–1

Thoppil P G and Hogan P J 2010a Persian Gulf response to a wintertime shamal wind event *Deep-Sea Research Part I: Oceanographic Research Papers* **57** 946–55

Thoppil P G and Hogan P J 2010b Persian Gulf response to a wintertime shamal wind event *Deep Sea Res. Part I* **57** 946–55

Vasou P, Vervatis V, Krokos G, Hoteit I and Sofianos S 2020 Variability of water exchanges through the strait of Hormuz *Ocean Dyn.* **70** 1053–65

Wang X, Peng S, Liu Z, Huang R X, Qian Y-K and Li Y 2015 Tidal mixing in the South China Sea: An estimate based on the internal tide energetics *J. Phys. Oceanogr.* **46** 107–24

Xue P and Eltahir E A 2015 Estimation of the heat and water budgets of the Persian (Arabian) gulf using a regional climate model *J. Clim.* **28** 5041–62

Yao F and Johns W E 2010 A HYCOM modeling study of the Persian Gulf: 1. Model configurations and surface circulation *Journal of Geophysical Research: Oceans* **10** C12038